Bioorganic & Medicinal Chemistry Letters 21 (2011) 2394–2399

Contents lists available at ScienceDirect

Bioorganic & Medicinal Chemistry Letters

journal homepage: www.elsevier.com/locate/bmcl

Discovery of 2,4-bis-arylamino-1,3-pyrimidines as insulin-like growth factor-1 receptor (IGF-1R) inhibitors

John L. Buchanan [a,*], John R. Newcomb [d], David P. Carney [b], Stuart C. Chaffee [a], Lilly Chai [d], Rod Cupples [h], Linda F. Epstein [c], Paul Gallant [b], Yan Gu [c], Jean-Christophe Harmange [a], Kathy Hodge [b], Brett E. Houk [e], Xin Huang [c], Janan Jona [g], Smriti Joseph [g], H. Toni Jun [d], Rakesh Kumar [d], Chun Li [e], John Lu [d], Tom Menges [e], Michael J. Morrison [b], Perry M. Novak [a], Simon van der Plas [a], Robert Radinsky [d], Paul E. Rose [c], Satin Sawant [f], Ji-Rong Sun [d], Sekhar Surapaneni [e], Susan M. Turci [d], Keyang Xu [e], Evelyn Yanez [g], Huilin Zhao [c], Xiaotian Zhu [c]

[a] Department of Medicinal Chemistry, Amgen Inc., 360 Binney Street, Cambridge, MA 02142, USA
[b] Department of HTS & Molecular Pharmacology, Amgen Inc., 360 Binney Street, Cambridge, MA 02142 and Amgen Inc., One Amgen Center Drive, Thousand Oaks, CA 91320, USA
[c] Department of Molecular Structure, Amgen Inc., 360 Binney Street, Cambridge, MA 02142, USA
[d] Department of Oncology Research, Amgen Inc., 360 Binney Street, Cambridge, MA 02142 and Amgen Inc., One Amgen Center Drive, Thousand Oaks, CA 91320, USA
[e] Department of Pharmacokinetics and Drug Metabolism, Amgen Inc., One Amgen Center Drive, Thousand Oaks, CA 91320, USA
[f] Department of Toxicology, Amgen Inc., One Amgen Center Drive, Thousand Oaks, CA 91320, USA
[g] Department of Pharmaceutics, Amgen Inc., One Amgen Center Drive, Thousand Oaks, CA 91320, USA
[h] Department of Metabolic Disorders, Amgen Inc., One Amgen Center Drive, Thousand Oaks, CA 91320, USA

ARTICLE INFO

Article history:
Received 11 August 2010
Revised 16 February 2011
Accepted 17 February 2011
Available online 23 February 2011

Keywords:
Insulin-like growth factor-1 receptor
IGF-1R
Kinase
Pyrimidine
Calu-6 xenograft
X-ray cocrystal structure

ABSTRACT

The insulin-like growth factor-1 receptor (IGF-1R) plays an important role in the regulation of cell growth and differentiation, and in protection from apoptosis. IGF-1R has been shown to be an appealing target for the treatment of human cancer. Herein, we report the synthesis, structure–activity relationships (SAR), X-ray cocrystal structure and in vivo tumor study results for a series of 2,4-bis-arylamino-1,3-pyrimidines.
© 2011 Elsevier Ltd. All rights reserved.

The insulin-like growth factor-1 receptor (IGF-1R) belongs to the insulin family of growth factors and receptors, and includes the insulin receptor (InsR), insulin-like growth factors 1 and 2 (IGF-1 and IGF-2), and six insulin-like growth factor binding proteins (IGFBP). Activation of IGF-1R by IGF-1 or IGF-2 leads to activation of both the Ras/Raf/MEK/ERK and PI3K/Akt/mTOR pathways, promoting proliferation and inhibiting apoptosis.[1] Conversely, inhibition of IGF-1R results in decreased proliferation of tumor cells and therefore represents an attractive oncology drug target. To date, IGF-1R is well established as an oncology drug target with a number of small molecules and antibodies currently undergoing clinical trials, including ganitumab (AMG 479).[2] The rationale for targeting the IGF-1R pathway as well as early results from these clinical trials have been well reviewed.[3] In parallel with our antibody efforts, we initiated a small molecule drug discovery program. Herein we disclose the discovery of 2,4-bis-arylamino-1,3-pyrimidines as IGF-1R inhibitors.

Screening of our kinase-preferred collection identified a number of hits for our small molecule program. Among those hits were many from the 2,4-bis-arylamino-1,3,5-triazine class of compounds[4] where several showed modest potency in our enzyme[5] (double-digit nM) and cellular[6] assays (~1 μM). More focused screening identified triazines **1** and **2** as preferred compounds from this series (Table 1). Replacement of the triazine core (X = N) in **1** and **2** with the pyrimidine[7] core (X = CH) in **3** and **4** resulted in a marked improvement in enzyme and cellular potency. This improvement in potency can be explained by the pyrimidine CH's enhanced compatibility with the adjacent hydrophobic

* Corresponding author. Tel.: +1 617 444 5031; fax: +1 617 621 3907.
E-mail address: john.buchanan@amgen.com (J.L. Buchanan).

0960-894X/$ - see front matter © 2011 Elsevier Ltd. All rights reserved.
doi:10.1016/j.bmcl.2011.02.075

Table 1
Initial assessment of screening hits **1** and **2** (IC_{50}, nM)[a]

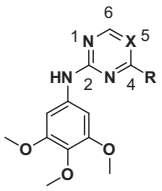

	X	R	IGF-1R IC_{50}	huIGF-1R/3T3 IC_{50}
1	N	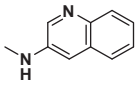	41	175
2	N	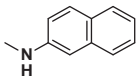	13	409
3	CH	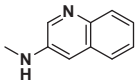	2.5	19
4	CH	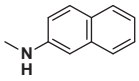	2.2	88
5	CH	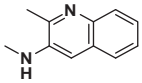	48	420
6	CH	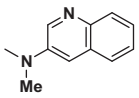	725	
7	CH	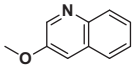	933	

[a] IC_{50} values are means of two or more separate determinations, in duplicate.

environment (vide infra). Based on these results, additional optimization efforts on 2,4-bis-arylamino-1,3-pyrimidines were undertaken.

The effects of additional minor changes around the central core can be found in Table 1. Addition of a methyl group on the quinoline ring (**5**) resulted in a loss in both enzyme and cellular potency relative to quinoline **3**. Replacement of the 4-position N–H with either N–Me (**6**) or O (**7**) resulted in a significant loss in enzyme potency. These results can be explained by examining the cocrystal structure of pyrimidine **8** (Table 3) bound to IGF-1R (Fig. 1).

As shown in Figure 1, pyrimidine **8** (Table 3) binds to unphosphorylated IGF-1R (IGF-1R0P) in a U-shaped conformation.[8] Key interactions between pyrimidine **8** and IGF-1R include the typical donor–acceptor–donor triad interaction with the hinge region. Met1082 donates a backbone N–H to the pyrimidine N1 acceptor (3.08 Å) while its carbonyl accepts the pyrimidine 2-position N–H (3.00 Å). The carbonyl of Glu1080 accepts the pyrimidine 6-position C–H (2.92 Å). The pyrimidine 4-position N–H interacts with Asp1153 from the DFG motif of the activation loop (3.07 Å). Disruption of this interaction occurs in **5** resulting in a modest loss in potency. The importance of this interaction is demonstrated more markedly in the significant loss of potency seen in both N–Me analog **6** and ether **7**. The side chain of the gatekeeper Met1079 is positioned adjacent to the pyrimidine 5-position (3.63 Å), explaining the preference for pyrimidine (CH) over triazine (N). Additionally, the side chain of Met1156 from the DFG motif of the activation loop sits directly below the quinoline ring

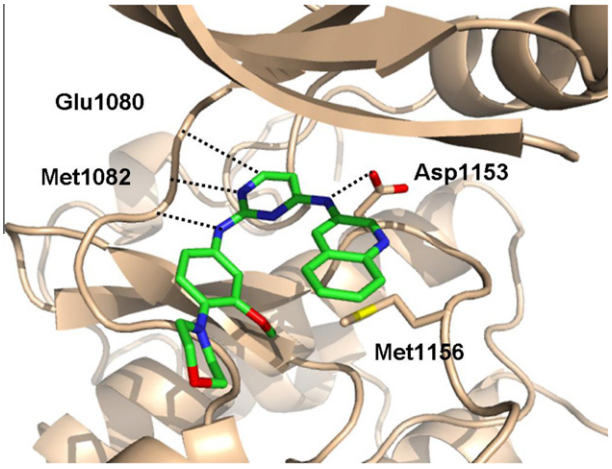

Figure 1. Cocrystal structure of pyrimidine **8** in IGF-1R0P.

making important hydrophobic interactions between its CH_3 and the quinoline bridging carbons (3.41 and 3.30 Å) and between its CH_2 and the quinoline nitrogen atom (3.35 Å). The sulfur atom serves to position the CH_3–CH_2 carbons appropriately. Finally, the morpholine group on the aniline ring is directed toward the solvent front, while the adjacent methoxy group occupies a hydrophobic region formed by the side chains of Met1156 (3.20 Å) and Met1142 (3.49 Å).

At this point, we decided to expand our examination of the structure–activity relationships (SAR), focusing first on the pyrimidine 4-position. Several bicyclic ring replacements were examined, many of which displayed desirable enzyme and cellular potency as demonstrated by isoquinoline **9** and quinoline **10** (Table 2). Insertion of an additional nitrogen atom into quinoline **10** provided quinoxaline **11** which showed reduced potency. NH-containing bicyclic ring replacements such as indazoles **12** and **13**, benzimidazole **14** and indoline **15** resulted in significant losses in potency. Attempts to replace the bicyclic ring with pyridyl (**16**) and/or substituted phenyl (**17**) rings resulted in reduced enzyme and cellular potency as compared to quinoline **3**. The loss in potency resulting from decreasing the lipophilicity of the bicyclic ring (**11**–**15**) or from excising the outer ring (**16** vs **9**) demonstrated the importance of the hydrophobic interactions between the side chain of Met1156 and the quinoline-type bicyclic rings.

We next turned our attention to the pyrimidine 2-position, fixing the 4-position with 3-aminoquinoline while examining the results of modifications to the trimethoxyaniline (Table 3).[9] The removal of methoxy groups from compound **3**, resulted in losses in both enzyme and cellular potency as exemplified by dimethoxy (**18**, **19**) and monomethoxy (**20**, **21**) arylamines. Modification of the methoxy group of **21** to trifluoromethoxy resulted in a significant loss in potency (**22**). 3-Chloro arylamine **23** displayed similar enzyme potency but slightly reduced cellular potency when compared to 3-methoxy arylamine **21**. Incorporation of a methoxy group at the 4-position of **23** afforded **24** which exhibited improved cellular potency. Guided by the observation that substituents at the 4-position of these arylamines were directed toward the solvent front, we decided to incorporate several solubilizing substituents in lieu of the methoxy at the 4-position toward improving cellular potency[10] and decreasing O-demethylation.[9] Toward this end, morpholine-containing compound **25** and tethered piperidine analog **26** displayed improved cellular shifts as compared to other 4-substituted arylamines (i.e., **20**). Introduction of the 3-methoxy group to **25** provided **8** which resulted in

Table 2
SAR of pyrimidine 4-position substituents (IC_{50}, nM)[a]

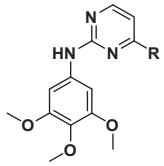

	R	IGF-1R IC_{50}	huIGF-1R/3T3 IC_{50}
3	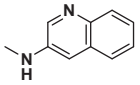	2.5	19
9	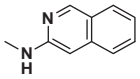	5.2	14
10	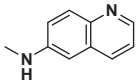	3.3	37
11	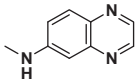	58	448
12	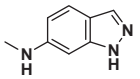	103	9219[b]
13	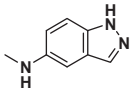	34	5121
14	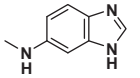	201	4221
15	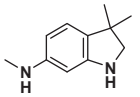	123	490
16	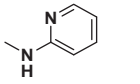	251	
17	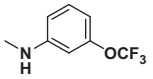	30	1651[b]

[a] IC_{50} values are means of two or more separate determinations, in duplicate.
[b] huIGF-1R/Rat1 proliferation IC_{50}.

single digit nM enzyme and cellular potency. Introduction of the 3-methoxy group to **26** afforded **27**, which displayed improved enzyme potency with a slight improvement in cellular potency. The improvements in potency demonstrated by compounds **8** and **27** supports the importance of the hydrophobic interaction of the 3-methoxy group with the Met1156 and Met1142 side chains as shown in the cocrystal structure of **8** and IGF-1R (Fig. 1).

Based on their in vitro profiles, several pyrimidines were selected for rat pharmacokinetic (PK) studies.[11] Pyrimidine 4-position analogs **4**, **9** and **13** (Tables 1 and 2) were cleared at rates near or greater than hepatic blood flow (2.4–4.7 L/h/kg). Pyrimidine 2-position analogs **19**, **24** and **8** (Table 3) were also cleared at rates near or greater than hepatic blood flow (2.9–9.5 L/h/kg). Compound **27** displayed some improvement, but was cleared at a rate of 1.9 L/h/kg. In contrast, lower clearance rates and generally improved PK properties were observed with trimethoxyaniline-containing quinolines **10** and **3** and tethered piperidine **26** (Table 4). Compound **3** exhibited a low clearance rate (0.4 L/h/kg) and acceptable oral bioavailability (33%)

Table 3
SAR of pyrimidine 2-position substituents (IC_{50}, nM)[a]

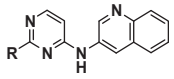

	R	IGF-1R IC_{50}	huIGF-1R/3T3 IC_{50}
3	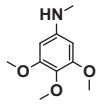	2.5	19
18	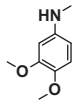	18	507
19	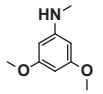	20	6453[b]
20	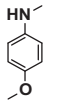	55	17383
21		40	1044
22		198	
23		41	3377
24	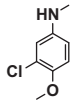	36	356
25	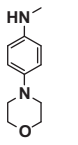	22	177
26	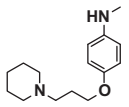	19	81
8	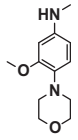	2.4	8.4
27	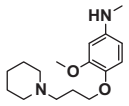	3.8	36

[a] IC_{50} values are means of two or more separate determinations, in duplicate.
[b] huIGF-1R/Rat1 proliferation IC_{50}.

Table 4
Rat pharmacokinetics for selected compounds[a]

	iv/po dose (mg/kg)	CL (L/h/kg)	V_{ss} (L/kg)	$T_{1/2}$ (h)	F (%)
10	1/5	1.2	1.1	1.3	16
3	1/5	0.4	0.2	1.7	33
26	2/5	0.6	9.5	12.1	9

[a] Dosed as a solution in DMSO (iv) or as a suspension (po) in 1% Tween 80 and 1% HPMC in water.

Table 5
Mouse pharmacokinetics for selected compounds[a]

	iv/po dose (mg/kg)	CL (L/h/kg)	V_{ss} (L/kg)	$T_{1/2}$ (h)	F (%)
10	1/5	6.4	1.8	2.3	56
3	1/5	1.6	0.3	1.7	63
26	12/30	5.9	28.1	5.3	30

[a] Dosed as a solution in DMSO (iv) or as a suspension (po) in 20% captisol in PBS for **3** and **10**. Dosed in aqueous propylene glycol (iv) or as a suspension in 20% captisol in PBS (pH 5.73) for **26**.

compared to compound **10**. Compound **26** also displayed a low clearance rate (0.6 L/h/kg) but much lower bioavailability (9%). In contrast to compounds **3** and **10**, compound **26** had a very large volume of distribution (9.5 L/kg) and a long half-life ($T_{1/2}$ = 12.1 h).

In preparation for a mouse Calu-6 tumor xenograft study, trimethoxyaniline-containing quinolines **10** and **3** as well as tethered piperidine **26** were evaluated in mouse PK studies (Table 5). Oral bioavailability was observed for all three compounds, with compound **3** displaying an acceptable clearance rate but a low volume of distribution. Compound **26** displayed a high clearance rate (5.9 L/h/kg) and a very large volume of distribution (28.1 L/kg) which in turn led to an extended half-life ($T_{1/2}$ = 5.3 h).

Based on its cellular potency and oral bioavailability in the mouse, compound **3** was chosen to be evaluated in a mouse Calu-6 tumor xenograft model.[12] Upon dosing up to 100 mg/kg b.i.d. for 35 days, compound **3** showed no effect on tumor growth (Table 6) nor was there any change in blood glucose levels or body weight (data not shown). Terminal PK studies revealed a low plasma concentration of **3** (unbound <200 nM at 100 mg/kg b.i.d.). In addition, compound **3** had poor tumor distribution (AUC tumor/AUC plasma <0.2).[13]

Anticipating that the high V_{ss} and long $T_{1/2}$ displayed by compound **26** would result in greater tumor exposure, compound **26** was also evaluated in the mouse Calu-6 tumor xenograft model. Upon dosing up to 100 mg/kg b.i.d. for 28 days, compound **26** displayed 56% tumor growth inhibition (TGI), comparable to 49% TGI demonstrated by the commercial IGF-1R antibody mAb391[14,15] (Table 6). In this Letter, a 200 mg/kg b.i.d. dose was not tolerated.[16] There was no change in blood glucose levels for either dose of compound **26** or for mAb391 (data not shown).[17a] Terminal PK studies demonstrated much higher tumor exposure at 100 mg/kg as well as a large tumor/plasma ratio (AUC tumor/AUC plasma >80) in contrast to that seen for **3** (Table 6).[13]

Tumors were assessed for levels of IGF-1R phosphorylation by a semi-quantitative western blot analysis that showed that compound **26** inhibited autophosphorylation of IGF-1R ~80% compared to controls at the efficacious dose (100 mg/kg) but not at the lower dose (30 mg/kg). In addition, compound **26** presented no significant effect on blood glucose levels following insulin and glucose challenges up to 200 mg/kg (data not shown).[17b]

Table 7
Kinase selectivity data for compounds **3** and **26**

Kinase	**3** IC_{50}[a] (μM)	Sel. ratio	**26** IC_{50}[a] (μM)	Sel. ratio
IGF-1R	0.0025	1	0.019	1
InsR	0.0030	1	0.024	1
AurA1	>5	>2000	>5	>263
CDK2	0.711	284	19.5	1026
cMet	2.11	844	8.99	473
EGFR	0.853	341	2.29	121
FGFR	1.58	632	4.53	238
KDR	0.094	38	1.37	72
Tie2	0.746	298	4.13	217

[a] IC_{50} values are means of two or more separate determinations, in duplicate.

Select kinase selectivity data for compounds **3** and **26** can be found in Table 7. Compound **26** displayed good selectivity compared to a number of kinases involved in tumor cell growth and differentiation. All compounds tested were equipotent with respect to IGF-1R versus InsR.[18,19]

The relative ease of synthesis of the 2,4-bis-arylamino-1,3-pyrimidines[7] is illustrated in Scheme 1.[20] The sequential addition of amines occurs first at the pyrimidine 4-position followed by the pyrimidine 2-position. For example, 3-aminoquinoline was added to a solution of 2,4-dichloropyrimidine in the presence of Hunig's base in *i*-PrOH and the mixture was heated overnight, giving the intermediate chloropyrimidine **28**. Following purification, the addition of 3,4,5-trimethoxyaniline in DMSO at 100 °C led to aminoquinoline **3**. Alkylation of piperidine with 1-bromo-3-chloropropane provided the intermediate chloride which was used in the alkylation of 4-nitrophenol giving **29**. Reduction of the nitro group in **29** afforded amine **30** which was then added to the intermediate chloropyrimidine **28** as described earlier to give **26**. Finally, morpholine was coupled to the commercially available bromide **31** using standard conditions.[21] Reduction of the nitro group in **32** provided amine **33** which could be added to intermediate chloropyrimidine **28** to afford **8**.

In summary, we have discovered a series of potent, orally bioavailable IGF-1R inhibitors. Pyrimidine **26** displayed tumor growth inhibition in vivo in a mouse Calu-6 tumor xenograft model with comparable activity to mAb391. An X-ray cocrystal structure was obtained and revealed key binding elements of this series of compounds and provided suggestions for further optimization. Results from these optimization efforts will be reported in due course.

Table 6
In vivo antitumor activity against Calu-6 tumor xenografts implanted subcutaneously in mice

		C_{max} plasma (μM)	C_{max} plasma (fu)[c] (μM)	C_{max} tumor (μM)	AUC tumor (h ng/mL)	AUC tumor/AUC plasma	TGI %
3	30 mg/kg[a]	5.34	0.0748	0.525	989	0.129	0
3	100 mg/kg[a]	13.4	0.188	2.72	5174	0.180	0
26	30 mg/kg[a]	0.18	0.0018	1.36	13,271	11.6	0
26	100 mg/kg[a]	2.22	0.0189	142.9	1,118,319	81.9	56[d]
mAb391	300 μg[b]						49[e]

[a] b.i.d.
[b] Twice per week.
[c] Mouse plasma protein binding (**3** = 98.6%; **26** = 99.15%).
[d] p = 0.046.
[e] p = 0.033.

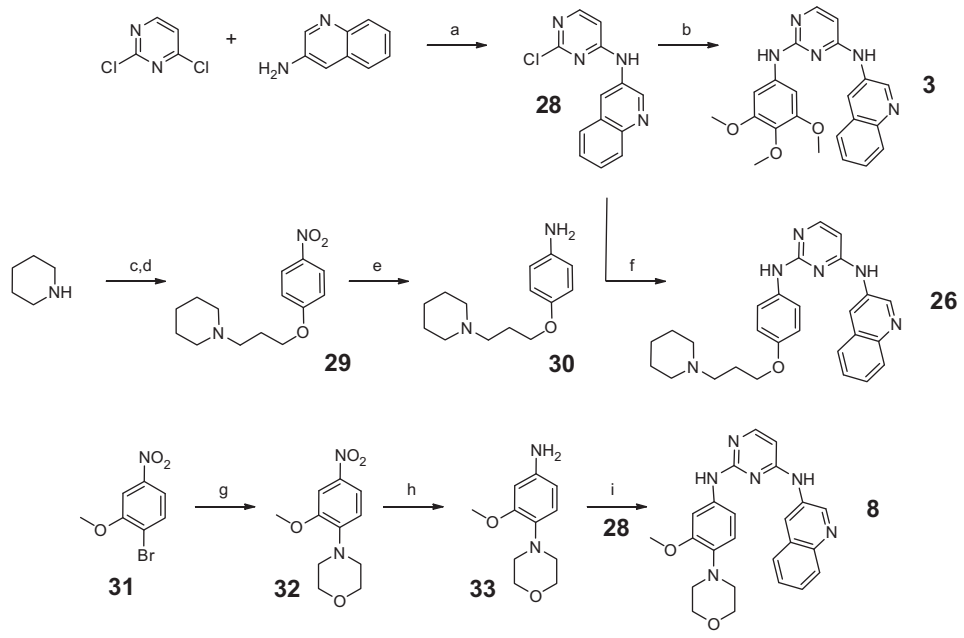

Scheme 1. Synthesis of 2,4-bis-arylamino-1,3-pyrimidines **3**, **26**, and **8**. Reagents and conditions: (a) *i*-Pr_2NEt, *i*-PrOH, 100 °C, 12 h, 40%; (b) 3,4,5-trimethoxyaniline, DMSO, 100 °C, 65%; (c) 1-bromo-3-chloropropane, THF, rt, 67%; (d) *p*-nitrophenol, K_2CO_3, DMF; (e) H_2, Pd/C, rt, 86% (two steps); (f) **28**, DMSO, 100 °C, 33%; (g) morpholine, $Pd_2(dba)_3$, NaO*t*-Bu, BINAP, $PhCH_3$, 80 °C, 3 h, 66%; (h) H_2, Pd/C, EtOH, rt; (i) **28**, DMSO, 100 °C.

Acknowledgments

The authors thank Nick Lydon, David Armistead, Rick Kendall, Murray Robinson, Dave Lacey, Joe Kim and Vinod Patel for their support of this research program. We thank Jean Bemis for providing compound **17**, Lucian DiPietro for providing compounds **1** and **2**, Pedro Beltran for help with statistics and Erin DiMauro and Margaret Chu-Moyer for helpful discussions.

References and notes

1. Pollak, M. N.; Schernhammer, E. S.; Hankinson, S. E. *Nat. Rev. Cancer* **2004**, *4*, 505. and references cited therein.
2. (a) Tolcher, A. W.; Sarantopoulos, J.; Patnaik, A.; Papadopoulos, K.; Lin, C.-C.; Rodon, J.; Murphy, B.; Roth, B.; McCaffery, I.; Gorski, K. S.; Kaiser, B.; Zhu, M.; Deng, H.; Friberg, G.; Puzanov, I. *J. Clin. Oncol.* **2009**, *23*, 5800; (b) Beltran, P. J.; Mitchell, P.; Chung, Y.-A.; Cajulis, E.; Lu, J.; Belmontes, B.; Ho, J.; Tsai, M. M.; Zhu, M.; Vonderfecht, S.; Baserga, R.; Kendall, R.; Radinsky, R.; Calzone, F. J. *Mol. Cancer Ther.* **2009**, *8*, 1095.
3. (a) Wittman, M. D.; Velaparthi, U.; Vyas, D. M. *Ann. Rep. Med. Chem.* **2009**, *44*, 281; (b) Li, R.; Pourpak, A.; Morris, S. W. *J. Med. Chem.* **2009**, *52*, 4981; (c) Hewish, M.; Chau, I.; Cunningham, D. *Recent Patents Anti-Cancer Drug Discov.* **2009**, *4*, 54; (d) Gualberto, A.; Pollak, M. *Oncogene* **2009**, *28*, 3009; (e) Ryan, P. D.; Goss, P. E. *Oncologist* **2008**, *13*, 16; (f) Rodon, J.; DeSantos, V.; Ferry, R. J., Jr.; Kurzrock, R. *Mol. Cancer Ther.* **2008**, *7*, 2575; (g) Chitnis, M. M.; Yuen, J. S. P.; Protheroe, A. S.; Pollak, M.; Macaulay, V. M. *Clin. Cancer Res.* **2008**, *14*, 6363; (h) Hubbard, S. R.; Miller, W. T. *Curr. Opin. Cell Biol.* **2007**, *19*, 117; (i) Imai, K.; Takaoka, A. *Nat. Rev. Cancer* **2006**, *6*, 714; (j) Yuen, J. S. P.; Macaulay, V. M. *Expert Opin. Ther. Targets* **2008**, *12*, 589; (k) Weroha, S. J.; Haluska, P. *J. Mammary Gland Biol. Neoplasia* **2008**, *13*, 471; (l) Paz, K.; Hadari, Y. R. *Comb. Chem. High Throughput Screening* **2008**, *11*, 62; (m) Wang, Y.; Ji, Q.-S.; Mulvihill, M.; Pachter, J. A. *Recent Results Cancer Res.* **2007**, *172*, 59; (n) Hubbard, R. D.; Wilsbacher, J. L. *ChemMedChem* **2007**, *2*, 41; (o) Hartog, H.; Wesseling, J.; Boezen, H. M.; van der Graaf, W. T. A. *Eur. J. Cancer* **2007**, *42*, 1895; (p) Clemmons, D. R. *Nat. Rev. Drug Disc.* **2007**, *6*, 821; (q) Sarma, P.; Tandon, R.; Gupta, P.; Dastidar, S. G.; Ray, A.; Das, B.; Cliffe, I. A. *Expert Opin. Ther. Patents* **2007**, *17*, 25; (r) Garcia-Echeverria, C. *IDrugs* **2006**, *9*, 415; (s) Hofmann, F.; Garcia-Echeverria, C. *Drug Discovery Today* **2005**, *10*, 1041; (t) Zhang, H.; Yee, D. *Expert Opin. Invest. Drugs* **2004**, *13*, 1569.
4. Armistead, D. M.; Bemis, J. E.; Buchanan, J. L.; DiPietro, L. V.; Elbaum, D.; Habgood, G. J.; Kim, J. L.; Marshall, T. L.; Geuns-Meyer, S. D.; Novak, P. M.; Nunes, J. J.; Patel, V. F.; Toledo-Sherman, L. M.; Zhu, X. WO 01/25220.
5. All compounds were screened in a homogeneous time-resolved fluorescence (HTRF) kinase assay at the apparent K_m of ATP with respect to 1 μM of peptide substrate.
6. (a) Human tumor cell lines or a rat fibroblast cell line were plated out in flat-well plates in complete medium and allowed to adhere overnight. The cells were then starved in medium containing 0.1% bovine serum albumin (BSA) overnight, pre-incubated for 1 h with or without dilutions of compound, then activated overnight with 50 ng/mL insulin-like growth factor (IGF-1). Proliferation was determined by the level of ^{3}H-thymidine incorporation into DNA. IC_{50}'s were determined by comparing the level of thymidine incorporation found in the presence of compound compared to controls. (b) Compounds were routinely assessed in an assay measuring IGF-1-induced auto-phosphorylation of IGF-1Rβ and displayed good correlation with the proliferation results.
7. (a) Armistead, D. M.; Bemis, J. E.; DiPietro, L. V.; Geuns-Meyer, S. D.; Habgood, G. J.; Kim, J. L.; Nunes, J. J.; Patel, V. F.; Toledo-Sherman, L. M. WO 01/60816.; (b) Buchanan, J. L.; Chaffee, S.; Harmange, J.-C.; Novak, P. M.; Zhu, X. WO 03/018022.; (c) Harmange, J.-C.; Booker, S.; Buchanan, J. L.; Chaffee, S.; Novak, P. M.; Van Der Plas, S.; Zhu, X. WO 03/018021.
8. The kinase domain of human IGF-1R (res 988 to 1286) with an N-terminal GST tag was expressed in insect cells and purified by immobilized glutathione affinity, anion exchange, and size exclusion chromatographies. The coordinates for the X-ray co-crystal structure of IGF-1R and **8** have been deposited in the PDB. The RCSB ID code is RCSB063987 and the PDB ID code is 3QQU.
9. Incubation of **3** with rat or human liver microsomes in the presence of NADPH identified O-demethylation as a major route of metabolism.
10. This strategy to improve cellular potency has been previously reported, for example: Martin, M. W.; Newcomb, J.; Junes, J. J.; Boucher, C.; Chai, L.; Epstein, L. F.; Faust, T.; Flores, S.; Gallant, P.; Gore, A.; Gu, Y.; Hsieh, F.; Huang, X.; Kim, J. L.; Middleton, S.; Morgenstern, K.; Oliveira-dos-Santos, A.; Patel, V. F.; Powers, D.; Rose, P.; Tudor, Y.; Turci, S. M.; Welcher, A. A.; Zack, D.; Zhao, H.; Zhu, L.; Zhu, X.; Ghiron, C.; Ermann, M.; Johnston, D.; Saluste, C.-G. P. *J. Med. Chem.* **2008**, *51*, 1637.
11. (a) Male Sprague–Dawley rats were administered a solution of compound in DMSO at the indicated doses iv For oral dosing, a suspension of the compound in 1% Tween 80 and 1% HPMC in water was administered. Samples were collected over a 12–24 h period and analyzed for parent compound by LC–MS. (b) In vitro clearance (RLM and MLM) was not predictive of in vivo clearance, thus compounds were chosen for PK studies based on their enzyme and cellular potency profiles.
12. Calu-6 cell lines were obtained originally from ATCC and were maintained in RPMI 1640 10% FBS, 1 × NEAA, 2 mM L-glutamine (Gibco/BRL, Grand Island, NW). CD1 mice within approximately 4–8 weeks were challenged with subcutaneous injections of Calu-6 (human NSCLC) cells (5×10^6 cells per mouse). After 1 day, animals began continuous daily treatment with compound administered po, b.i.d at the indicated dose levels in 1% Tween 80 and 1% HPMC in water (**3**) or in 20% Captisol in PBS at pH 3.5 (**26**). Tumor volumes as established by caliper measurements were recorded twice per week, along with body weights as an index of toxicity. Blood glucose levels were recorded before dosing and once per week. Data are expressed as mean values plus or minus standard errors as a function of time. Statistical significance of observed differences was evaluated by repeated measures

analysis of variance (RMANOVA) followed by Scheffe post hoc testing for multiple comparisons.

13. IC_{50}'s were determined for **3** (0.110 μM) and **26** (0.69 μM) in a Calu-6 proliferation assay.[6,12] Proliferation assays are performed under serum-starved conditions, hindering the typical calculation of target coverage. The total tumor concentration for **3** was 25-fold higher than the cellular IC_{50} at the high dose (100 mg/kg). The total tumor concentration for **26** at the efficacious dose (100 mg/kg) was 207-fold higher than the Calu-6 cellular IC_{50}, while only 2-fold higher at the lower dose (30 mg/kg). Using mouse plasma protein binding to estimate free concentration in tumors, the efficacious dose of **26** (100 mg/kg b.i.d.) was the only dose which achieved a concentration (1.2 μM) higher (1.8-fold) than the IC_{50} (0.69 μM) determined in the Calu-6 proliferation assay.
14. (a) Hailey, J.; Maxwell, E.; Koukouras, K.; Bishop, W. R.; Pachter, J. A.; Wang, Y. *Mol. Cancer Ther.* **2002**, *1*, 1349; (b) 300 μg was chosen based on the maximal effect shown in an engineered IGF-1R-dependent 32D tumor xenograft model (Refs. 2b and 15). Data not shown.
15. Peruzzi, F.; Prisco, M.; Dews, M.; Salomoni, P.; Grassilli, E.; Romano, G.; Calabretta, B.; Baserga, R. *Mol. Cell. Biol.* **1999**, *19*, 7203.
16. Higher doses (200 mg/kg b.i.d.) were tolerated in an engineered IGF-1R-dependent 32D tumor xenograft study (Refs. 2b and 15), but were not tolerated in the longer term Calu-6 xenograft study. Data not shown.
17. (a) Blood glucose levels were checked at day 0, 9 and 21 within the Calu-6 xenograft study. No significant changes in blood glucose levels outside of the normal range were observed. (b) An insulin challenge test was done within the Calu-6 xenograft at day 17 of dosing. No significant differences were noted (at either the 30 or 100 mg/kg doses) in the ability of the animals to respond to insulin by modulating blood glucose. It is possible that at the 100 mg/kg dose of compound **26**, the level of insulin receptor inhibition is not complete enough to result in metabolic effects.
18. Recent data suggests that the inhibition of both IGF-1R and InsR may be desirable. See for example: (a) Pollak, M. *Nat. Rev. Cancer* **2008**, *8*, 915; (b) Zhang, H.; Fagan, D. H.; Zeng, X.; Freeman, K. T.; Sachdev, D.; Yee, D. *Oncogene* **2010**, *29*, 2517; (c) Buck, E.; Gokhale, P. C.; Koujak, S.; Brown, E.; Eyzaguirre, A.; Tao, N.; Rosenfeld-Franklin, M.; Lerner, L.; Chiu, M. I.; Wild, R.; Epstein, D.; Pachter, J. A.; Miglarese, M. R. *Mol. Cancer Ther.* **2010**, *9*, 1349.
19. Clinical results for two advanced small molecule dual IGF-1R/InsR inhibitors in the clinic should help define the importance of InsR inhibition. See for example: (a) Wittman, M. D.; Carboni, J. M.; Yang, Z.; Lee, F. Y.; Antman, M.; Attar, R.; Balimane, P.; Chang, C.; Chen, C.; Discenza, L.; Frennesson, D.; Gottardis, M. M.; Greer, A.; Hurlburt, W.; Johnson, W.; Langley, D. R.; Li, A.; Li, J.; Liu, P.; Mastalerz, J.; Mathur, A.; Menard, K.; Patel, K.; Sack, J.; Sang, X.; Saulnier, M.; Smith, D.; Stefanski, K.; Trainor, G.; Velaparthi, U.; Zhang, G.; Zimmermann, K.; Vyas, D. M. *J. Med. Chem.* **2009**, *52*, 7360; (b) Carboni, J. M.; Wittman, M.; Yang, Z.; Lee, F.; Greer, A.; Hurlburt, W.; Hillerman, S.; Cao, C.; Cantor, G. H.; Dell-John, J.; Chen, C.; Discenza, L.; Menard, K.; Li, A.; Trainor, G.; Vyas, D.; Kramer, R.; Attar, R. M.; Gottardis, M. M. *Mol. Cancer Ther.* **2009**, *8*, 3341; (c) Mulvihill, M. J.; Cooke, A.; Rosenfeld-Franklin, M.; Buck, E.; Foreman, K.; Landfair, D.; O'Connor, M.; Pirritt, C.; Sun, Y.; Yao, Y.; Arnold, L. D.; Gibson, N. W.; Ji, Q.-S. *Future Med. Chem.* **2009**, *1*, 1153.
20. All new compounds were characterized by mass spectroscopy and ^{1}H NMR and were determined to be of >95% purity by reverse phase HPLC.
21. Wolfe, J. P.; Wagaw, S.; Buchwald, S. L. *J. Am. Chem. Soc.* **1996**, *118*, 7215.